

Design of three-groove kinematic couplings

Alexander H. Slocum

Department of Mechanical Engineering, Massachusetts Institute of Technology, Cambridge, MA, USA

Kinematic couplings are statically determinant structures that are often used in precision fixturing applications because of their high repeatability. The simplicity of their design also makes the design of accurate interchangeable couplings a realistic task. This paper discusses three-groove kinematic coupling design methodologies and then describes the theory required to calculate stresses at the contact interfaces and error motions at any point on the coupling. The theory presented is incorporated into a kinematic coupling design spreadsheet (written in Microsoft Excel) that can run on a personal computer.

Keywords: *kinematic; coupling; fixturing*

Introduction

Kinematic couplings have long been known to provide an economical and dependable method for attaining high repeatability in fixtures.¹ Properly designed kinematic couplings are deterministic: They only make contact at a number of points equal to the number of degrees of freedom that are to be restrained. Being deterministic makes performance predictable and also helps to reduce design and manufacturing costs.² On the other hand, contact stresses in kinematic couplings are often very high, and no elastohydrodynamic lubrication layer exists between the elements that are in point contact: thus for high cycle applications, it is advantageous to have the contact surfaces made from corrosion-resistant materials (e.g., ceramics). When nonstainless steel components are used, one must be wary of fretting at the contact interfaces so steel couplings should only be used for low cycle applications.

Tests on a heavily loaded (80% of allowable contact stress) steel ball/steel groove system have shown that 0.1 μm repeatability can be attained³; however, with every cycle of use, the repeatability worsened until an overall repeatability on the order of 10 μm was reached after several hundred cycles. At this point, fret marks were observed at the contact points. Tests on a heavily loaded (80% of allowable contact stress) silicon nitride/steel groove system have shown that 50 nm repeatability could be attained

over a range of a few dozen cycles, and that with continued use the overall repeatability asymptotically approached the surface finish of the grooves (on the order of $1/3 \mu\text{m } R_a$). An examination of the contact points showed an effect akin to burnishing, but once the coupling had worn in, 0.1 μm repeatability was ultimately obtained. Unfortunately, references were not found in the literature that make an extensive comparison of the effects of load and surface finish on kinematic coupling repeatability.

The tests that were reported also showed that with the use of polished corrosion resistant (preferably ceramic) surfaces, a heavily loaded kinematic coupling can easily achieve 0.1 μm and better repeatability with little or no wear-in required. Regrettably, too many designers still consider kinematic couplings to be useful only for instrument or metrology applications. Therefore, this paper is presented to describe in detail the analysis tools needed to design kinematic couplings for any application. The analysis tools presented are also implemented on a spreadsheet (written in Microsoft Excel).*

Coupling configuration and stability

Symmetry aids in reducing manufacturing costs, and for practical fixturing applications in general, the use of grooves for all contact regions minimizes the overall stress state in the coupling. Thus, it is assumed here that the kinematic coupling to be designed is a three-groove type.

Two forms of three-groove couplings are illustrated in Figure 1. Planar couplings are often found in

Address reprint requests to Dr. Alexander H. Slocum, Department of Mechanical Engineering, Massachusetts Institute of Technology, Room 35-008, 77 Massachusetts Ave., Cambridge, MA 02139, USA.

This paper was written while the author was at the Automated Production Technology Division of the National Institute of Standards and Technology, Gaithersburg, MD, USA.

© 1992 Butterworth-Heinemann

* The spreadsheet is being distributed by the American Society for Precision Engineering, Box 7918, Raleigh, NC 27695-7918, USA (919-737-3096).

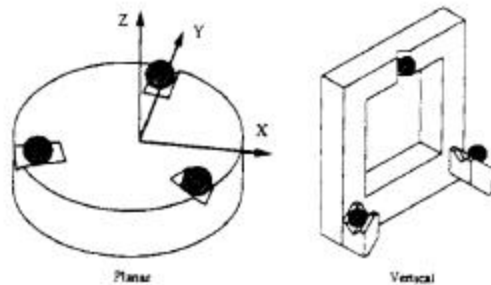


Figure 1 Examples of three-groove kinematic couplings for horizontal and vertical fixturing applications. The coupling components to which the balls are permanently affixed are not shown for clarity

metrology applications. They can also be used in the manufacture of precision parts. For example, a planar coupling can be used to hold a grinding fixture on a profile grinder. A matching three-groove plate on a coordinate measuring machine allows the grinding fixture to be transferred to the coordinate measuring machine with the part. The part can be measured and then placed back onto the grinder so the errors can be corrected. To minimize Abbe errors in some applications, vertically oriented couplings can be designed where the preload is obtained with a clamping mechanism or by gravity acting on a mass held by a cantilevered arm. An example would be a three-groove kinematic coupling used to hold photolithographic masks in a wafer stepper whose projection axis must be horizontal because of its size.

With three grooves, the question naturally arises as to what is the best orientation for the grooves. Mathematically, to guarantee that the coupling will be stable, James Clerk Maxwell stated the following⁴:

When an instrument is intended to stand in a definite position on a fixed base it must have six bearings, so arranged that if one of the bearings

were removed the direction in which the corresponding point of the instrument that would be left free to move by the other bearings must be as nearly as possible normal to the tangent plane at the bearing.

(This condition implies that, of the normals to the tangent planes at the bearings, no two coincide; no three are in one plane, and either meet in a point or are parallel; no four are in one plane, or meet in a point, or are parallel, or, more generally, belong to the same system of generators of an hyperboloid of one sheet. The conditions for five normals and for six are more complicated.)

In a footnote to this discussion, Maxwell references Sir Robert Ball's pioneering work in *screw theory*. Screw theory asserts that the motion of any system can be represented by a combination of a finite number of screws of varying pitch that are connected in a particular manner. This concept is well illustrated for a plethora of mechanisms by Phillips.⁵ Ball's work on screws spanned the latter half of the 19th century, and a detailed summary of his work on screw theory was published in 1900.⁶ Ball's treatise describes the theory of screws in elegant, yet easily comprehensible, linguistic and mathematical terms. Currently, research in automation is attempting to use screw theory to determine what is the best way to grasp an object (e.g., with a robotic hand) or to fixture a part (e.g., for automated fixture design for manufacturing).^{7†}

Screw theory is an elegant and powerful tool for analyzing the motion of rigid bodies in contact, but it is not always easy to apply. Fortunately, designers of precision kinematic couplings are not faced with the

[†] This reference summarizes work done by John Bausch for his Ph.D. thesis in the Mechanical Engineering Department at MIT. Dr. Slocum, who was a member of Bausch's thesis committee, first suggested to Bausch that screw theory would provide a good theoretical method for studying the problem of automated fixture design.

Notation			
c, d	major and minor semiaxis of contact region ellipse	ξ_{B_i}	the coordinates of the contact points of the balls in the grooves ($\xi = x, y, z$)
F_{B_i}	the normal contact forces between the balls and the grooves	ξ_{P_i}	the coordinates of up to three preload forces ($\xi = x, y, z$)
F_{L_i}	the magnitudes of the external applied load ($\xi = x, y, z$)	ξ_L	the coordinates of an external applied load ($\xi = x, y, z$)
F_{P_i}	the preload forces' magnitudes ($\xi = x, y, z$)	γ_{B_i}	contact forces' direction cosines ($\xi = x, \beta, \gamma$)
E_{ball}	modulus of elasticity of the ball material	x, β, γ	Hertz contact stress analysis parameters
E_{groove}	modulus of elasticity of the groove material	δ	Hertz contact deflection: approach of two far field points
E_e	equivalent modulus of elasticity	δ_{z_c}	translational error motions ($\xi = x, y, z$) of the coupling centroid
$L_{i,c}$	distance from ball i to the coupling centroid	ϵ_i	rotational error motions ($\xi = x, y, z$) of the coupling
$L_{i,jk}$	distance from ball i to side jk	θ_{ij}	slope angle of the coupling triangle's side ij
q	contact pressure	η_{ball}	Poisson's ratio of the ball material
R_e	equivalent radius	η_{groove}	Poisson's ratio of the groove material
R_1	ball radius		
R_2	groove radius		

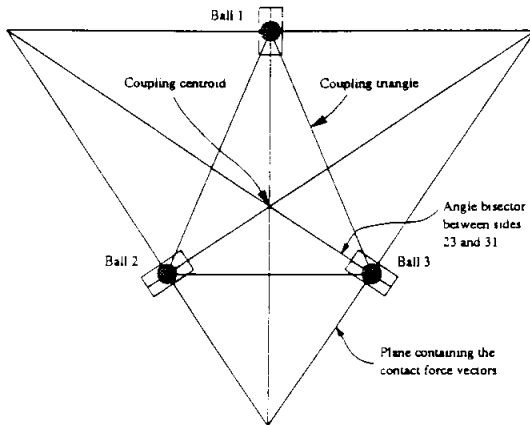


Figure 2 For good stability in a three-groove kinematic coupling, the normals to the planes containing the contact force vectors should bisect the angles between the balls

generic grasp-a-potato problem faced by researchers in robotics. Thus, with respect to practical implementation of the theoretical requirement for stability, for precision three-groove kinematic couplings, stability and good overall stiffness will be obtained if the normals to the plane of the contact force vectors bisect the angles of the triangle formed by the hemispheres (e.g., balls) that lie in the grooves.‡ Furthermore, for balanced stiffness in all directions, the contact force vectors should intersect the plane of coupling action at an angle of 45°. The angle bisector concept is illustrated in Figure 2. Note that the angle bisectors intersect at a point that is also the center of the circle that can be inscribed in the coupling triangle. This point is referred to as the *coupling centroid*, and it is only coincident with the coupling triangle's centroid when the coupling triangle is an equilateral triangle.

For a coupling where the balls lie on the vertices of an equilateral triangle, the angle bisectors also intersect at the triangle's centroid. If the normals to the planes containing the contact forces' vectors were to always point toward the coupling triangle's centroid instead of along its angle bisectors, then the coupling's stiffness will decrease as the coupling triangle's aspect ratio increases. This concept is illustrated in Figure 3. Most coupling designs seek to obtain good stiffness in all directions; however, in some cases it may be desirable to maximize the stiffness in a particular direction.

Note that any three-groove kinematic coupling's stability can be quickly assessed by examining the intersections of the planes that contain the contact force vectors. For stability, the planes must form a triangle as illustrated in Figure 4.

‡ From conversations and observations with Dr. William Plummer, Director of Optical Engineering, Polaroid Corp., 38 Henry Street, Cambridge, MA 02139, USA.

Analysis of three-groove couplings

Figure 5 illustrates the information needed to characterize a three-groove kinematic coupling. In order to design a three-groove kinematic coupling, the designer must provide the following information:

- The balls' diameters and the grooves' radii of curvature.
- The coordinates x_{B_i} , y_{B_i} , and z_{B_i} of the contact points of the balls in the grooves.
- The contact forces' direction cosines α_{B_i} , β_{B_i} , and γ_{B_i} .
- The coordinates x_{P_i} , y_{P_i} , and z_{P_i} of up to three preload forces.
- The x , y , and z direction preload forces' magnitudes F_{P_i} at each of the three points.
- The coordinates x_L , y_L , and z_L of an external applied load (the effect of more loads can be evaluated using superposition).
- The x , y , and z direction magnitudes F_{L_i} of the externally applied load.
- The moduli of elasticity and Poisson ratios of the ball and groove materials.

The following is the output from the analysis:

- The contact forces (F_{B_i}).
- The contact stresses.
- The deflections at the contact points.
- The six error motion terms (δ_x , δ_y , δ_z , ϵ_x , ϵ_y , ϵ_z) that exist at the coupling's centroid.

Force and moment equilibrium

The force and moment balance equations for the system are

$$\sum_{i=1}^6 F_{B_i} \alpha_{B_i} + \sum_{i=1}^3 F_{P_i} + F_{L_x} = 0 \quad (1)$$

$$\sum_{i=1}^6 F_{B_i} \beta_{B_i} + \sum_{i=1}^3 F_{P_i} + F_{L_y} = 0 \quad (2)$$

$$\sum_{i=1}^6 F_{B_i} \gamma_{B_i} + \sum_{i=1}^3 F_{P_i} + F_{L_z} = 0 \quad (3)$$

$$\sum_{i=1}^6 F_{B_i} (-\beta_{B_i} z_{B_i} + \gamma_{B_i} y_{B_i}) + \sum_{i=1}^3 (-F_{P_i} z_{P_i} + F_{P_i} y_{P_i}) - F_{L_y} z_L + F_{L_z} y_L = 0 \quad (4)$$

$$\sum_{i=1}^6 F_{B_i} (\alpha_{B_i} z_{B_i} - \gamma_{B_i} x_{B_i}) + \sum_{i=1}^3 (F_{P_i} z_{P_i} - F_{P_i} x_{P_i}) - F_{L_x} z_L - F_{L_z} x_L = 0 \quad (5)$$

$$\sum_{i=1}^6 F_{B_i} (-\alpha_{B_i} y_{B_i} + \beta_{B_i} x_{B_i}) + \sum_{i=1}^3 (-F_{P_i} y_{P_i} + F_{P_i} x_{P_i}) - F_{L_x} y_L + F_{L_y} x_L = 0 \quad (6)$$

Slocum: Three-groove kinematic couplings

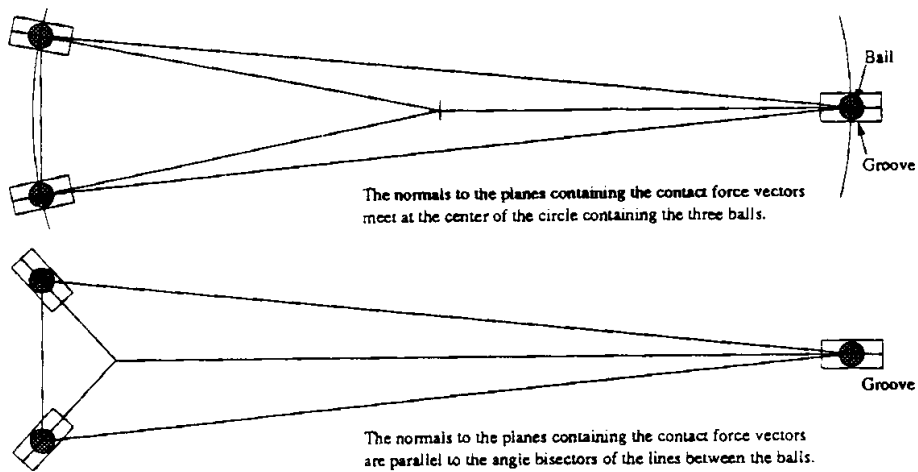


Figure 3 Consider the design of a long coupling to locate a laser head on an instrument. Compare the stability of couplings designed by two methods that give the same solution for a coupling where the balls lie on the vertices of an equilateral triangle

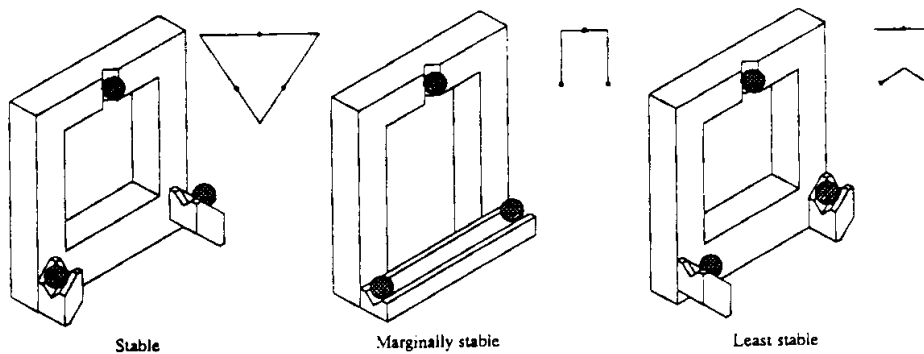


Figure 4 Different configurations for a kinematic coupling that illustrate how the intersections of the planes containing the contact force vectors can be used to make an assessment of the coupling's stability

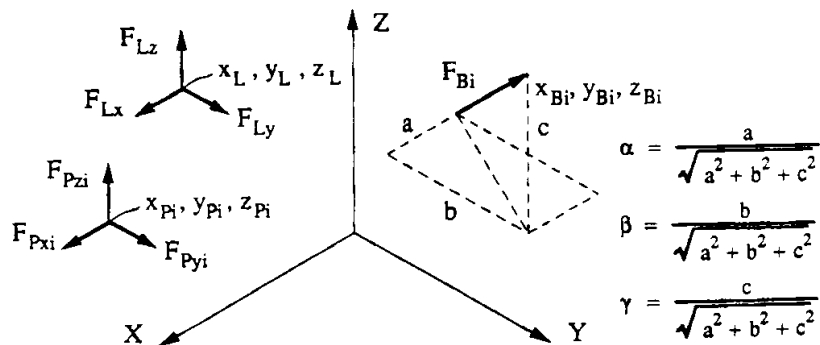


Figure 5 Information required to define a three-groove kinematic coupling

The magnitudes of the six contact point forces are easily calculated using a spreadsheet. Once the magnitudes of the forces are known, they can be used to determine the stress and deflection at the contact points using Hertz theory.

Stress and deflection at the contact points

The accuracy of Hertz theory for determining the stress and deflection of two bodies in point contact has been verified many times.⁸ For the purposes of implementing Hertz theory on a spreadsheet used for design of kinematic couplings, the following calculations need to be made⁹: First, the equivalent modulus of elasticity must be determined for each of the contact points:

$$E_e = \frac{1}{\frac{1 - \nu_{ball}^2}{E_{ball}} + \frac{1 - \nu_{groove}^2}{E_{groove}}} \quad (7)$$

Next, the equivalent radius of the system is found:

$$R_e = \frac{1}{\frac{1}{R_{1\ major}} + \frac{1}{R_{1\ minor}} + \frac{1}{R_{2\ major}} + \frac{1}{R_{2\ minor}}} \quad (8)$$

For the ball, $R_{1\ major} = R_{1\ minor}$ and both numbers have a positive value. For the groove, $R_{2\ major} = \infty$, and $R_{2\ minor}$ has a negative value.

The factor $\cos \theta$ is determined, which in the general case (e.g., two crossed cylinders) takes into account the angle ϕ between the bodies:

$$\begin{aligned} \cos \theta = R_e & \left[\left(\frac{1}{R_{1\ major}} - \frac{1}{R_{1\ minor}} \right)^2 \right. \\ & + \left(\frac{1}{R_{2\ major}} - \frac{1}{R_{2\ minor}} \right)^2 \\ & + 2 \left(\frac{1}{R_{1\ major}} - \frac{1}{R_{1\ minor}} \right) \\ & \left. \times \left(\frac{1}{R_{2\ major}} - \frac{1}{R_{2\ minor}} \right) \cos 2\phi \right]^{1/2} \quad (9) \end{aligned}$$

For the case of a ball in a groove, Equation 9 reduces to $R_e / |R_{2\ minor}|$.

The factor $\cos \theta$ is used in the evaluation of functions of elliptic integrals whose values have been tabulated for most engineering applications of Hertz theory. The functions are referred to as α , β , and λ , and when plotted over the full range of values given, it is virtually impossible to fit curves to the data. In order to facilitate the incorporation of α , β , and λ into a spreadsheet, only the values of α , β , and λ for $\cos \theta$ from 0.0–0.9 are used. This incorporates most coupling groove designs and allows for the following polynomial

approximations to be made with less than about 5% error:

$$\begin{aligned} \alpha = & 0.99672 + 1.2786 \cos \theta - 6.7201 \cos^2 \theta \\ & + 27.379 \cos^3 \theta - 41.827 \cos^4 \theta \\ & + 23.472 \cos^5 \theta \quad (10) \end{aligned}$$

$$\begin{aligned} \beta = & 1.0000 - 0.68865 \cos \theta + 0.58909 \cos^2 \theta \\ & - 1.3277 \cos^3 \theta + 1.7706 \cos^4 \theta \\ & - 0.99887 \cos^5 \theta \quad (11) \end{aligned}$$

$$\begin{aligned} \lambda = & 0.75018 - 0.042126 \cos \theta + 0.29526 \cos^2 \theta \\ & - 1.7567 \cos^3 \theta + 2.6781 \cos^4 \theta \\ & - 1.5533 \cos^5 \theta \quad (12) \end{aligned}$$

The contact region will be an ellipse, where the major and minor semiaxis, respectively

$$c = \alpha \left(\frac{3FR_e}{2E_e} \right)^{1/3} \quad d = \beta \left(\frac{3FR_e}{2E_e} \right)^{1/3} \quad (13)$$

The contact pressure is given by

$$q = \frac{3F}{2\pi cd} \quad (14)$$

The contact pressure can be used to evaluate the state of stress below the surface. For most applications, one can merely specify an allowable contact pressure for a given material. The deflection (distance of approach of two far field points in the bodies) is given by

$$\delta = \lambda \left(\frac{2F^2}{3R_e E_e^2} \right)^{1/3} \quad (15)$$

Note that this assumes that the ball is effectively a hemisphere. In other words, the ball must be attached to one part of the coupling in a manner that makes deformation of the attachment zone negligible compared with the deformation of the contact region.

Kinematics of the coupling's error motions

The contact between the ball and the groove actually results in an elastic indentation of the region. Combined with a finite coefficient of friction, it is reasonable to assume that there is no relative motion between the ball and the groove at the contact interface. If one makes this assumption and then calculates the new position of the balls' centers using the contact displacements and contact forces' direction cosines, then one finds that there is not a unique homogeneous transformation matrix that relates the old and new ball positions. These factors make the calculation of a kinematic coupling's error motions a nondeterministic problem.

Fortunately, if the distances between the balls, determined using their new coordinates, do not change greatly, then reasonable estimates can be made of the coupling's error motions. Using the design theory presented herein, a spreadsheet can be used to show that the change in distance between the balls is typically five to ten times less than the deflection at

⁹ The reader may also want to consider another means of approximating Hertz contact stresses. See D. E. Brewe and B. J. Hamrock, "Simplified solution for elliptical-contact deformation between two elastic solids," *J. Lubrication Tech.*, 1977, Trans ASME, Series F, 99, 485–487.

the contact points. Furthermore, the ratio of the change in the distance between the balls to the distance between the balls is typically an order of magnitude less than the ratio of the deflection of the ball to the ball diameter (see the calculations in Appendix A). Thus, estimates of the coupling's error motions can be made in the following manner:

- The product of the deflection of the balls with the contact forces' direction cosines are used to calculate the ball's deflections. The displacements of the coupling triangle's centroid, δ_{ic} ($i = x, y, z$), are assumed to be equal to the weighted average (by the distance between the balls and the coupling centroid) of the ball's deflections:

$$\delta_{ic} = \left(\frac{\delta_{1i}}{L_{1c}} + \frac{\delta_{2i}}{L_{2c}} + \frac{\delta_{3i}}{L_{3c}} \right) \frac{L_{1c} + L_{2c} + L_{3c}}{3} \quad (16)$$

- The rotations of the coupling about the X- and Y-axes are conveniently determined for the case of a coupling whose grooves lie in the X-Y plane (other orientations confuse the angle definition in the spreadsheet analysis). To determine the rotations, the altitudes of the coupling triangle and its sides' orientation angles must be determined as shown in Figure 6. With these geometric calculations, the rotations about the X- and Y-axes can be determined:

$$\epsilon_x = \frac{\delta_{z1}}{L_{1,23}} \cos \theta_{23} + \frac{\delta_{z2}}{L_{2,31}} \cos \theta_{31} + \frac{\delta_{z3}}{L_{3,12}} \cos \theta_{12} \quad (17)$$

$$\epsilon_y = \frac{\delta_{z1}}{L_{1,23}} \sin \theta_{23} + \frac{\delta_{z2}}{L_{2,31}} \sin \theta_{31} + \frac{\delta_{z3}}{L_{3,12}} \sin \theta_{12} \quad (18)$$

- The coupling's rotation about the Z-axis is assumed to be the average of the rotations about the Z-direction through the coupling centroid

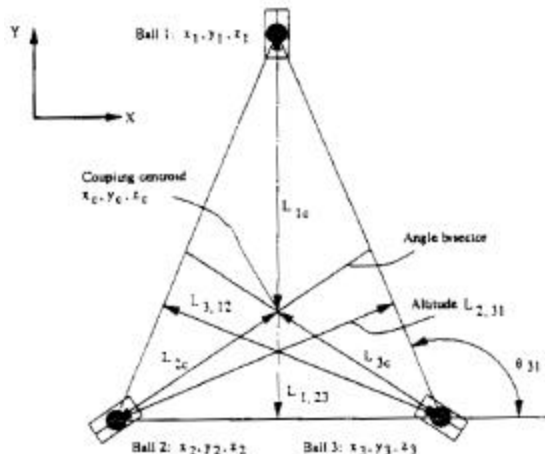


Figure 6 Geometry of a planar kinematic coupling

calculated for each ball. For example, the rotation about a Z-direction through the coupling centroid caused by ball 1 is

$$\epsilon_{z1} = \frac{\sqrt{(x_{B1}\delta_1 + x_{B2}\delta_2)^2 + (\beta_{B1}\delta_1 + \beta_{B2}\delta_2)^2}}{\sqrt{(x_1 - x_c)^2 + (y_1 - y_c)^2}} \times \text{SIGN}(x_{B1}\delta_1 + x_{B2}\delta_2) \quad (19)$$

The rotation error about the Z-axis of the coupling is assumed to be

$$\epsilon_z = \frac{\epsilon_{z1} + \epsilon_{z2} + \epsilon_{z3}}{3} \quad (20)$$

The errors can then be assembled into a homogeneous transformation matrix for the coupling that allows for the determination of the translational errors δ_x , δ_y , and δ_z at any point x , y , or z in space around the coupling:

$$\begin{bmatrix} \delta_x \\ \delta_y \\ \delta_z \\ 1 \end{bmatrix} = \begin{bmatrix} 1 & -\epsilon_z & \epsilon_y & \delta_x \\ \epsilon_z & 1 & -\epsilon_x & \delta_y \\ -\epsilon_y & \epsilon_x & 1 & \delta_z \\ 0 & 0 & 0 & 1 \end{bmatrix} \begin{bmatrix} x - x_c \\ y - y_c \\ z - z_c \\ 1 \end{bmatrix} \quad (21)$$

In the homogeneous transformation matrix it has been assumed that the rotations are small, so small angle trigonometric approximations are valid. Also, the error motions had been calculated about the coupling triangle's centroid, which may not be coincident with the coordinate system's origin; hence, the centroid coordinates are subtracted from the location at which the errors are to be determined.

Practical design considerations

With a spreadsheet, the design engineer can easily play "what if" design games to arrive at a theoretically workable kinematic coupling for virtually any application. However, the problem still remains: how to manufacture the coupling?

Silicon nitride or silicon carbide are the best materials for the spherical parts of the coupling. Either balls or cylinders with a hemispherical end can be used in the coupling. A cylinder with a spherical end can be pressed or epoxied into a hole to obtain near monolithic properties. Mounting of a ball takes more care to ensure that the compliance of the mounting method is very low compared with the compliance of

Standard size silicon nitride balls are available from Cerber Bearing Company, 10 Airport Road, East Granby, CT 06026, USA (203-653-8071). Cylinders with spherical ends can also be manufactured.

the coupling. Ball mounting methods include the following:

- A shaped seat can be machined, ground, or electrodischarge machined into the mounting surface for the ball. Shapes for the seat, in order of increasing compliance, include hemisphere, cone, and tetrahedron. For the hemisphere, the bottom of the hole should be counterbored to prevent contact of the ball near its pole, which would increase lateral compliance. For any of these seats, an extra same size ball should be burnished in place or pressed in until the surface is brinelled, which will help to ensure that the ball does not make contact at only two points in the case of a spherical or conical seat. A ball can then be brazed or epoxied into the seat to make the ball act as an integral part of the structure.
- A surface can be ground flat and then annular grooves ground around the ball locations. Sleeves can then be pressed into the grooves. The balls can then be pressed into the sleeves until they contact the flat surfaces. The balls should deeply brinell the flat surface in order to increase the bearing area and decrease the compliance.

With any of these methods, the difficulty in accurately locating the balls from fixture to fixture may suggest that the balls should be affixed to a rough machined fixture. The fixture would then be clamped to the grooved portion of the coupling and finish machined.

The ideal material for the grooves would also be a hard ceramic because it would not corrode, and the coefficient of friction between the ball and the groove would be minimized, which would maximize the repeatability of the coupling. The grooves can be profile ground in a monolithic plate using a profile grinder and an index table, or the grooves can be made in modular inserts that are bolted or bonded into place on the coupling.

Results and conclusions

The analysis methods described previously were implemented on a spreadsheet whose output is given

in Appendix A. The spreadsheet has a true/false option that allows the user to quickly enter data for a planar kinematic coupling where it is assumed that the grooves are spaced 120° apart and the direction cosines correspond to contact between the balls and the grooves at 45° angles with respect to the X-Y plane. When false is entered, the user must enter position and orientation data for each contact point. The spreadsheet always assumes that the centroid of the coupling is located where the angle bisectors of the coupling triangle meet.

In order to test the spreadsheet, forces were applied along axes of symmetry and it was checked to ensure that the expected displacements were obtained. For example, a Z-direction force should yield equal forces at all the contact points and only a Z displacement should occur. For all test cases, the results were as expected.

References

- 1 Evans, C. *Precision Engineering: An Evolutionary View*. Cranfield, England: Cranfield University Press, 1989, pp. 21–29
- 2 Slocum, A. "Kinematic couplings for precision fixturing – Part I – Formulation of design parameters." *Precision Engineering* 1988, 10, 85–91
- 3 Slocum, A. and Donmez, A. "Kinematic couplings for precision fixturing – Part II – Experimental determination of repeatability and stiffness." *Precision Engineering* 1988, 10, 115–121
- 4 Maxwell, J. C. "General considerations concerning scientific apparatus." in *The Scientific Papers of J. C. Maxwell*, vol. II, W. D. Niven, ed. London, England: Cambridge University Press, 1890, pp. 507–508
- 5 Phillips, J. *Freedom in Machinery*, vols. I and II. London, England: Cambridge University Press, 1982, p. 90
- 6 Ball, R. S. *A Treatise on the Theory of Screws*. London, England: Cambridge University Press, 1900
- 7 Bausch, J. J. and Youcef-Toumi, K. "Kinematic methods for automated fixture reconfiguration planning." *IEEE Conference on Robotics and Automation*, 1990, pp. 1396–1491
- 8 Seely, F. and Smith, J. *Advanced Mechanics of Materials*. New York: John Wiley & Sons, 1952
- 9 Young, W. *Roark's Formulas for Stress and Strain*, ed. 6. New York: McGraw-Hill, pp. 647–663

Appendix A

	A	B	C	D	E	F	G	H	
1	Appendix A								
2	Kinematic Coupling Design Spreadsheet								
3	Coupling geometry data								
4	XY plane is assumed to contain the ball centers								
5	For standard coupling designs, contact forces are inclined at 45 to the XY plane								
6	Standard 120 degree equal size groove coupling? TRUE								
7	For non standard designs, enter geometry after results section						Material properties		
8	Dball =	0.012	Ball diameter		Hertz stress				
9	Rgroove =	-1000000	Groove radius (negative for a trough)		SiNi		6.7500E+09		
10	Dcoupling =	0.100	Coupling diameter		96% Alumina		1.8559E+09		
11	Fpreload =	-1000	Preload force over each ball		RC 62 Steel		3.6225E+09		
12	Xerr =	0.000	X location of error reporting		Elastic modulus				
13	Yerr =	0.000	Y location of error reporting		SiNi		3.1050E+11		
14	Zerr =	0.000	Z location of error reporting		96% Alumina		3.0360E+11		
15	Auto select material values assume that metric units are used (mks)								
16	Matlab =	1	Enter 1 for SiN ball, SiN groove		Poisson ratio				
17			Enter 2 for SiN ball, Alumina groove		SiNi		0.27		
18			Enter 3 for SiN ball, RC 62 Fe groove		96% Alumina		0.21		
19			Enter 4 for RC 62 Fe ball, RC 62 Fe groove		RC 62 Steel		0.29		
20	Enter 5 for other values and enter them for each ball and groove								
21	Applied forces' Z,Y,Z values and coordinates			Coupling centroid		Effective K (N/micron)			
22	FLx =	90	XL =	0.000	xc	0.000	Fx/dx	210	
23	FLy =	0	YL =	0.000	yc	0.000	Fy/dy	FALSE	
24	FLz =	0	ZL =	0.000	zc	-0.017	Fz/dz	FALSE	
25	Results								
26	CAUTION: Groove normal force must be positive!								
27	Ball-Groove 1								
28	Groove normal forces		Contact stress		Stress/Allow		Deflection (+ into ball)		
29	Fbnone	7.50E+02	sigone	4.85E+09	0.72	delone	-4.70E-07		
30	Fbntwo	6.65E+02	sigtwo	4.66E+09	0.69	deltwo	4.80E-07		
31	Ball-Groove 2								
32	Groove normal forces		Contact stress		Stress/Allow		Deflection		
33	Fbthree	6.71E+02	sigthree	4.67E+09	0.69	delthree	4.12E-07		
34	Fbnfour	7.13E+02	sigfour	4.77E+09	0.71	delfour	-6.66E-08		
35	Ball-Groove 3								
36	Groove normal forces		Contact stress		Stress/Allow		Deflection		
37	Fbnfive	7.01E+02	sigfive	4.74E+09	0.70	delfive	6.68E-08		
38	Fbnsix	7.44E+02	sigsix	4.84E+09	0.72	delsix	-4.05E-07		
39	Error motions								
40	Error motions are at X,Y,Z coordinates:				0.000	0.000	0.000		
41	deltaX	4.28E-07							
42	deltaY	-2.31E-09		Homogenous Transformation Matrix:					
43	deltaZ	3.94E-09		1.00E+00	-8.96E-06	5.58E-06	3.36E-07		
44	EpsX	5.56E-08		8.96E-06	1.00E+00	-5.56E-08	-1.39E-09		
45	EpsY	5.58E-06		-5.58E-06	5.56E-08	1.00E+00	3.94E-09		
46	EpsZ	8.96E-06		0.00E+00	0.00E+00	0.00E+00	1.00E+00		
47	Generic data entry for non0120 degree couplings								
48	NOTE! For calculation of angular errors, the coupling is assumed to lie in the XY plane.								
49	Ball 1 must lie in quadrants 1 or 2, and Balls 2 & 3 must lie in quadrants 3 and 4								
50	Enter X,Y,Z coordinates and alpha, beta, gamma direction cosines for Ball 1								
51	Contact point 1				Contact point 2				
52	Xba =	0.004243		Xbb =	-0.004243				
53	Yba =	0.050000		Ybb =	0.050000				
54	Zba =	-0.025000		Zbb =	-0.025000				
55	Aba =	-0.707107		Abb =	0.707107				
56	Bba =	0.000000		Bbb =	0.000000				
57	Gba =	0.707107		Gbb =	0.707107				
58	Enter characteristics for groove 1 and ball 1								
59	Egone =	3.105E+11		Groove material elastic modulus					
60	vgone =	0.27		Groove material Poisson ratio					

	A	B	C	D	E	F	G	H
61	Rgone =	-1000000	Groove radius of curvature					
62	Ebone =	3.105E+11	Ball material elastic modulus					
63	νbone =	0.27	Ball material Poisson ratio					
64	Dbone =	0.012	Ball diameter					
65	Sone =	6.75E+09	Allowable Hertz stress					
66	Enter X,Y,Z coordinates and alpha, beta, gamma direction cosines for Ball 2							
67	Contact point 3			Contact point 4				
68	Xbc =	-0.045423	Xbd =	-0.041180				
69	Ybc =	-0.021326	Ybd =	-0.028674				
70	Zbc =	-0.025000	Zbd =	-0.025000				
71	Abc =	0.353553	Abd =	-0.353553				
72	Bbc =	-0.612372	Bbd =	0.612372				
73	Gbc =	0.707107	Gbd =	0.707107				
74	Enter characteristics for groove 2 and ball 2							
75	Egtwo =	3.105E+11	Groove material elastic modulus					
76	νgtwo =	0.27	Groove material Poisson ratio					
77	Rgtwo =	-1000000	Groove radius of curvature					
78	Ebtwo =	3.105E+11	Ball material elastic modulus					
79	νbtwo =	0.27	Ball material Poisson ratio					
80	Dbtwo =	0.012	Ball diameter					
81	Stwo =	6.75E+09	Allowable Hertz stress					
82	Enter X,Y,Z coordinates and alpha, beta, gamma direction cosines for Ball 3							
83	Contact point 5			Contact point 6				
84	Xbe =	0.041180	Xbf =	0.045423				
85	Ybe =	-0.028674	Ybf =	-0.021326				
86	Zbe =	-0.025000	Zbf =	-0.025000				
87	Abe =	0.353553	Abf =	-0.353553				
88	Bbe =	0.612372	Bbf =	-0.612372				
89	Gbe =	0.707107	Gbf =	0.707107				
90	Enter characteristics for groove 3 and ball 3							
91	Egthree =	3.105E+11	Groove material elastic modulus					
92	νgthree =	0.27	Groove material Poisson ratio					
93	Rgthree =	-1000000	Groove radius of curvature					
94	Ebthree =	3.105E+11	Ball material elastic modulus					
95	νbthree =	0.27	Ball material Poisson ratio					
96	Dbthree =	0.012	Ball diameter					
97	Stthree =	6.75E+09	Allowable Hertz stress					
98	Enter preload forces' X,Y,Z components and coordinates							
99	Fpxone =	0	Fpxtwo =	0	Fpxthree =	0		
100	Fpyone =	0	Fpytwo =	0	Fpythree =	0		
101	Fpzone =	-1000	Fpztwo =	-1000	Fpzthree =	-1000		
102	Xpone =	0	Xprtwo =	-0.04330127	Xprthree =	0.04330127		
103	Ypone =	0.05	Yprtwo =	-0.025	Yprthree =	-0.025		
104	Zpone =	0.024	Zprtwo =	0.024	Zprthree =	0.024		
105	Calculations:							
106	Build Force Moment equilibrium matrices: AF = B (Equations 1-6)							
107	Matrix A						Matrix F	B with loads
108	Fbn1	Fbn2	Fbn3	Fbn4	Fbn5	Fbn6		
109	-7.07E-01	7.07E-01	3.54E-01	-3.54E-01	3.54E-01	-3.54E-01	Fbn1	-9.00E+01
110	0.00E+00	0.00E+00	-6.12E-01	6.12E-01	6.12E-01	-6.12E-01	Fbn2	0.00E+00
111	7.07E-01	7.07E-01	7.07E-01	7.07E-01	7.07E-01	7.07E-01	Fbn3	3.00E+03
112	3.54E-02	3.54E-02	-3.04E-02	-4.97E-03	-4.97E-03	-3.04E-02	Fbn4	0.00E+00
113	1.47E-02	-1.47E-02	2.33E-02	3.80E-02	-3.80E-02	-2.33E-02	Fbn5	0.00E+00
114	3.54E-02	-3.54E-02	3.54E-02	-3.54E-02	3.54E-02	-3.54E-02	Fbn6	0.00E+00
115	Res. Forces with applied loads Res forces with preload only							
116	fbone	749.53	fone	707.11				
117	fbtwo	664.68	ftwo	707.11				
118	fbthree	670.64	ftthree	707.11				
119	fbfour	713.07	ffour	707.11				
120	fbfive	701.15	ffive	707.11				

Slocum: Three-groove kinematic couplings

	A	B	C	D	E	F	G	H
121	fbsix	743.57	fsix	707.11				
122	Original ball coordinates							
123	xboneO	0.000000	xbtwoO	-0.0433013	xbthreeO	0.0433013		
124	yboneO	0.0500000	ybtwoO	-0.0250000	ybthreeO	-0.0250000		
125	zboneO	-0.0165147	zbtwoO	-0.0165147	zbthreeO	-0.0165147		
126	New ball coordinates (=original + ball deflection*direction cosines)							
127	xboneN	0.0000007	xbtwoN	-0.0433011	xbthreeN	0.0433014		
128	yboneN	0.0500000	ybtwoN	-0.0250003	ybthreeN	-0.0249997		
129	zboneN	-0.0165147	zbtwoN	-0.0165145	zbthreeN	-0.0165150		
130	Ball centers' deflections							
131	dxone	6.72E-07	dxtwo	1.69E-07	dxthree	1.67E-07		
132	dyone	0.00E+00	dytwo	-2.93E-07	dythree	2.89E-07		
133	dzone	6.72E-09	dztwo	2.44E-07	dztthree	-2.39E-07		
134	Theory applicability check:							
135	Initial dist. between balls	Final dist. between balls		Difference				
136	Lotl	0.086603	LotN	0.086603	DLotl	-5.05E-07		
137	Ltll	0.086603	LtN	0.086603	DLtll	2.41E-09		
138	Ltol	0.086603	LtoN	0.086602	DLtol	5.03E-07		
139	Change in length/distance between balls		Deflection/ball radius		Ratio (must be >5)			
140	5.83E-06			8.00E-05		1.37E+01		
141	2.79E-08			6.86E-05		2.46E+03		
142	5.80E-06			6.75E-05		1.16E+01		
143	Coupling centroid is assumed to be at intersection of coupling triangle's angle bisectors							
144	Initial centroid	Distance from ball to centroid		Error motion at centroid from weighted ball motions				
145	xci	0.000000000	Dcone	0.050000000	dxcc	3.36E-07		
146	ycl	0.000000000	Dctwo	0.050000000	dyc	-1.39E-09		
147	zci	-0.016514719	Dctthree	0.050000000	dzc	3.94E-09		
148	Original angles between balls			Original altitude lengths				
149	Angone	60.0000	angle at ball 1	Aone	0.0750	Ball 1 to side 2 3		
150	Angtwo	60.0000	angle at ball 2	Atwo	0.0750	Ball 2 to side 1 3		
151	Angthree	60.0000	angle at ball 3	Athree	0.0750	Ball 3 to side 2 1		
152	New angles between balls			Original sides' angle with X axis				
153	AngoneN	60.0000	angle at ball 1	Aot	60	Side opposite ball 3		
154	AngtwoN	59.9994	angle at ball 2	Att	0	Side opposite ball 1		
155	AngthreeN	60.0006	angle at ball 3	Ato	120	Side opposite ball 2		
156	New sides' angle with X axis							
157	AotN	59.99980894	Side opposite ball 3					
158	AttN	0.000384816	Side opposite ball 1					
159	AtoN	119.9998062	Side opposite ball 2					
160	Original altitudes' slope angles and Y intercepts							
161	AmtwoO	30	AbtwoO	3.46945E-18				
162	AmtthreeO	150	AbthreeO	-3.46945E-18				
163	Rotation about opposite side (radians)							
164	Ttt	8.96E-08	rotation about side 23 due to Z motion at ball 1					
165	Tto	3.25E-06	rotation about side 13 due to Z motion at ball 2					
166	Tot	-3.19E-06	rotation about side 12 due to Z motion at ball 3					
167	Coupling error rotations							
168	EpsX	5.56E-08		EpsZ1	1.34E-05	Z rot from ball 1		
169	EpsY	5.58E-06		EpsZ2	6.76E-06	Z rot from ball 2		
170	EpsZ	8.96E-06		EpsZ3	6.67E-06	Z rot from ball 3		
171	Coupling HTM						Point of interest	
172	1.00E+00	-8.96E-06	5.58E-06	3.36E-07	Xerr	-5.78241E-20		
173	8.96E-06	1.00E+00	-5.56E-08	-1.39E-09	Yerr	-5.20417E-18		
174	-5.58E-06	5.56E-08	1.00E+00	3.94E-09	Zerr	0.016514719		
175	0.00E+00	0.00E+00	0.00E+00	1.00E+00	1	1		
176	Error displacements at the point of interest							
177	DeltaX	4.28E-07						
178	DeltaY	-2.31E-09						
179	DeltaZ	3.94E-09						
180		0						